$D^{*\pm}$ Production at high Q^2 with the H1 Detector

Martin Brinkmann* for the H1 Collaboration

University of Hamburg - Institute for Experimental Physics
Luruper Chaussee 149, D–22603 Hamburg - Germany

Inclusive production of $D^{*\pm}$-mesons in deep inelastic scattering at HERA is studied at high photon virtualities $100\,\mathrm{GeV}^2 < Q^2 < 1000\,\mathrm{GeV}^2$ for the first time with the H1 experiment [1]. The data were collected during the years 2004-2007 and correspond to an integrated luminosity of 351 pb^{-1}. Differential D^* production cross sections are measured and compared to predictions from the next-to-leading order program HVQDIS and the leading order Monte Carlo codes RAPGAP and CASCADE. The charm contribution $F_2^{c\bar{c}}$ to the proton structure function F_2 is extracted.

1 Introduction

Heavy flavour production in *ep* collisions at HERA is dominated by boson gluon fusion (BGF), i.e. $\gamma g \to Q\overline{Q}$, in leading order (LO) pQCD in the massive scheme. This process constrains the gluon density in the proton as demonstrated in previous analyses at lower photon virtuality Q^2 [2]. A proper treatment of charm and beauty quarks in pQCD models is one of the central issues in the determination of the parton distribution functions (PDFs) of the proton. Within the measurement of charm production at large photon virtualities the reliability of the pQCD calculations in the massive scheme for $Q^2 >> 4m_c^2$ is tested.

The current analysis uses data collected with the H1 detector [3] at HERA during the running periods of 2004-2007 when HERA operated with 27.5 GeV electrons and 920 GeV protons colliding at a centre of mass energy of $\sqrt{s} = 319\,\mathrm{GeV}$. The integrated luminosity for this analysis is $\mathcal{L} = 351\,\mathrm{pb}^{-1}$. Charm events are tagged via fully reconstructed $D^{*\pm}$-mesons using the decay chain $D^{*\pm} \to D^0 + \pi^{\pm}_{slow} \to K^{\mp} + \pi^{\pm} + \pi^{\pm}_{slow}$. $D^{*\pm}$-meson production cross sections are measured in the kinematic range of $100\,\mathrm{GeV}^2 < Q^2 < 1000\,\mathrm{GeV}^2$.

2 Theoretical models

The measured cross sections are compared to results from next-to-leading order (NLO) calculations in the *massive approach* provided by the HVQDIS program [4]. The calculations are done at fixed order with massive quarks assuming three active flavours in the proton. The heavy quarks are assumed to be produced at the perturbative level via BGF. The momentum densities of the three light quarks and the gluon in the proton are evolved by the DGLAP equations [5]. For the calculations the parton densities from the PDF set MRST2004FF3 [6] are used, the renormalisation and factorisation scale are set to $\mu_r = \mu_f = \mu_0 \equiv \sqrt{Q^2 + 4m_c^2}$ and a charm quark mass is chosen as $m_c = 1.43\,\mathrm{GeV}$. To obtain cross sections of $D^{*\pm}$-meson production the outgoing charm quarks are fragmented non-pertubatively into $D^{*\pm}$ mesons by using the Kartvelishvili *et al.* fragmentation function [7] with fragmentation parameters as measured by H1 [8]. To estimate the theoretical systematic uncertainty of the predicted cross sections the variations $1.3\,\mathrm{GeV} < m_c < 1.6\,\mathrm{GeV}$, $\mu_0/2 < \mu_r = \mu_f < 2\mu_0$ are done as well as the fragmentation parameter is varied within the experimental uncertainites [8].

*Supported by the German Federal Ministry of Science and Technology under grant 05H16GUA.

The data are also compared to calculations of the LO Monte Carlo (MC) programs RAPGAP [9] and CASCADE [10]. Both simulations are based on leading order matrix elements with the higher order corrections implemented via parton showers. Parton evolution according to the DGLAP [5] equations is used in the RAPGAP program with parton distribution functions according to the parametrisation set CTEQ65M [11]. CASCADE implies the intrinsic k_t factorisation and parton evolution according to the CCFM equations [12]. The parametrisation set A0 [13] is used for the unintegrated gluon distribution of the proton. In both MC models the fragmentation of quarks into hadrons is based on the Lund String model in case of light quarks and on the Bowler parametrisation for heavy quarks. The RAPGAP MC is also used to estimate the detector response using a full GEANT [14] based simulation of the H1 detector.

3 Experimental method

DIS events are selected by requiring the scattered electron in the liquid argon (LAr) calorimeter [15]. Together with the information from the hadronic final state (HFS), reconstructed from the corresponding tracker and calorimeter information the kinematic of the events is reconstructed where the following Lorentz invariant variables are used: the negative four-momentum squared Q^2 of the virtual photon, the Bjorken scaling variable x and the lepton inelasticity y.

Events with charm quarks are identified via full reconstruction of the decay chain $D^{*\pm} \rightarrow D^0 + \pi^{\pm}_{slow} \rightarrow K^{\mp} + \pi^{\pm} + \pi^{\pm}_{slow}$which has a branching ratio $\mathcal{B}$ of 2.57% [16]. The three tracks of the decay particles are reconstructed in the central track detector [17]. The cross section is measured in the visible range $100\,\mathrm{GeV}^2 < Q^2 < 1000\,\mathrm{GeV}^2$, $0.02 < y < 0.7$, $-1.5 < \eta(D^*) < 1.5$ and $p_t(D^*) > 1.5\,\mathrm{GeV}$.

In Fig. 1 the mass difference $\Delta m = m(K,\pi,\pi) - m(K,\pi)$ is shown for the complete data sample (points). A clear peak containing $N(D^*) = 497 \pm 37$ events is visible at the nominal $D^{*\pm} - D^0$ mass difference of 145.4 GeV.

The histogramm shows the wrong charge background obtained by requiring like sign charge $K\pi$ combinations associated with an oppositely charged π_{slow} candidate. The fit to the mass-difference distribution for the full sample assumes a symmetric Gauss-function for the signal and the Granet *et al.* parametrisation [18] for the background. The latter accounts for the characteristic power law behavior of the phase space at threshold and includes an exponential damping term to describe the behavior at larger values of Δm.

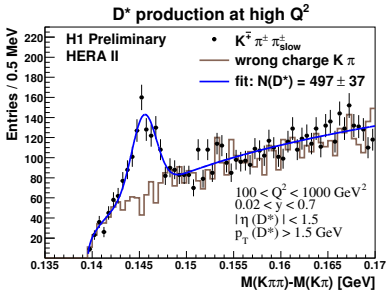

Figure 1: Distribution of the mass difference $m(K,\pi,\pi) - m(K,\pi)$ for $100\,\mathrm{GeV}^2 < Q^2 < 1000\,\mathrm{GeV}^2$

Visible D^* production cross sections are calculated as follows:

$$\sigma^{vis} = \frac{N(D^*)\,(1-R)}{\mathcal{L}\,\mathcal{B}(D^* \rightarrow K\pi\pi_s)\,\epsilon_{rec}\,(1-\delta_r)} \qquad (1)$$

Here $N(D^*)$ is the number of D^* obtained from fit to the Δm - distribution and ϵ_{rec} is

the total reconstruction efficiency determined using the RAPGAP Monte Carlo[a]. For this purpose the Monte Carlo was reweighted in Q^2 to better describe the measured differential cross-sections. R stands for the contribution of reflections in the D^0 mass window, coming from D^0 decay channels other than the one considered in this analysis. It amounts to $R = (4.4 \pm 0.5)\%$. The radiative corrections δ_r (less than 5 %) determined from Monte Carlo are applied to get the visible cross sections at the Born level.

4 Results

A total cross section in the visible range defined in Sec. 3 of

$$\sigma^{tot}_{vis}(e^{\pm}p \to e^{\pm}D^{*\pm}X) = 243 \pm 18\,(\text{stat.}) \pm 25\,(\text{syst.})\ \text{pb},$$

is observed. The prediction of the HVQDIS [4] program of

$$\sigma^{tot}_{vis}(e^{\pm}p \to e^{\pm}D^{*\pm}X) = 251\,^{+6}_{-7}\,(\text{model})\ \text{pb}.$$

is in good agreement with the data.

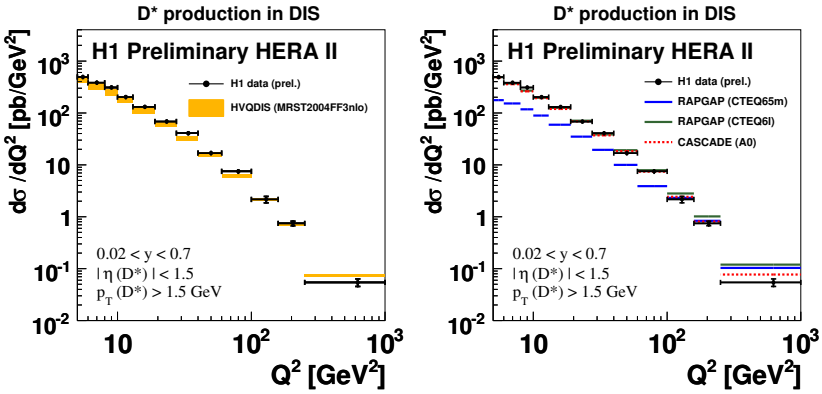

Figure 2: Differential cross sections as a function of Q^2 together with the result from the lower Q^2 analysis [19].

Fig. 2 shows the differential cross section as a function of Q^2 together with the result from the lower Q^2 analysis [19] in comparison with the NLO calculation (HVQDIS, left) and predictions from the LO MCs RAPGAP and CASCADE (right). The NLO calculation describes the Q^2 slope reasonably well over the full range.

RAPGAP with the parton density CTEQ6LL [20] describes the data at medium Q^2 well, while the PDF-set CTEQ65M [11] gives a better description of the high Q^2 data. Neither of the PDF-sets accounts for the slope over the full range in Q^2, since the PDFs were not consistently determined. In case of CASCADE which uses the consistently determined PDF set A0 the description is much better.

[a]The trigger efficiency is determined without Monte-Carlo simulation by inspecting independent triggers

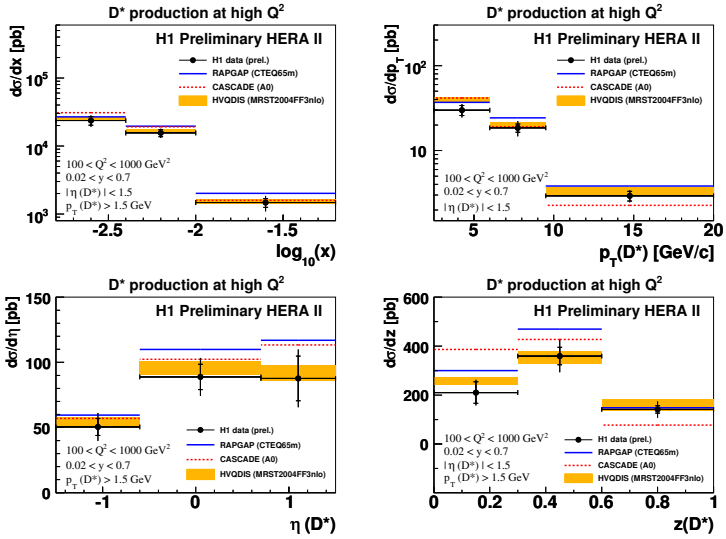

Figure 3: Differential cross sections as a function of x, $p_t(D^*)$, $\eta(D^*)$ and $z(D^*)$.

Figure 3 shows the measured differential cross sections as a function of $\log x$, $p_t(D^*)$, $\eta(D^*)$ and the fraction $z(D^*) = (E(D^*) - p_z(D^*))/(2yE_e)$ of the virtual photon momentum which is transferred to the D^*. These are compared to the Monte Carlo simulations RAPGAP [9] and CASCADE [10] and to the NLO calculation HVQDIS [4]. The latter describes all data distributions well, while RAPGAP and CASCADE give a poorer description, i.e. CASCADE fails to reproduce the cross sections in $p_t(D^*)$ and $z(D^*)$ and RAPGAP shows different dependencies in $\eta(D^*)$ and x than observed in data.

The double differential cross sections in Q^2 and x are used to extract F_2^c [21]. The extrapolation to the full phase space in $p_t(D^*)$ and $\eta(D^*)$ is done by HVQDIS with the parameters given in Sec. 2. The result is shown in Fig. 4. In the three highest Q^2 bins corresponding to this analysis the NLO calculation describes the data well.

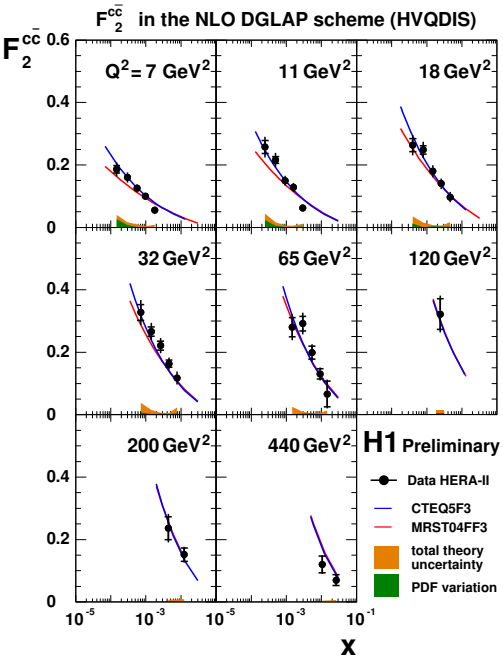

Figure 4: Extracted F_2^c

5 Conclusion

Cross sections of $D^{*\pm}$-meson production have been measured at photon virtualities $100\,\mathrm{GeV}^2 < Q^2 < 1000\,\mathrm{GeV}^2$. The cross sections were compared to the predictions from the LO MC programs RAPGAP and CASCADE and NLO calculations provided by HVQDIS. The NLO calculations describe the data well whereas the LO MCs shows deficiencies in some regions of the phase space. By extrapolating double differential cross sections in Q^2 and x to the full phase space $F_2^{c\bar{c}}$ has been extracted. The NLO calculations describe this measured quantity well.

References

[1] Slides:
`http://indico.cern.ch/contributionDisplay.py?contribId=170&sessionId=5&confId=53294`

[2] C. Adloff *et al.* (H1 Collaboration), Z. Phys. **C72** 593 (1996); C. Adloff *et al.* [H1-Collaboration], Nucl. Phys. **B545** 21 (1999); A. Aktas *et al.* [H1-Collaboration], Eur. Phys. J. **C51** 271 (2007).

[3] I. Abt *et al.* [H1 Collaboration], Nucl. Instrum. Meth. **A386** 310 (1997); ibid. 348.

[4] B. W. Harris and J. Smith, Phys. Rev. **D57** 2806 (1998); id. Nucl. Phys. **B452** 109 (1995); id. Phys. Lett. **B353** 535 (1995) [err. ibid **B359** 423 (1995)].

[5] V. Gribov, L. Lipatov, Sov. J. Phys. **15** 438 (1972), ibid. 675; L. Lipatov, Sov. J. Phys. **20** 94 (1975); G. Altarelli, G. Parisi, Nucl. Phys. **B126** 298 (1977); Y. Dokshitser, Sov. J. Phys. **46** 641 (1977).

[6] A.D. Martin, W.J. Stirling, and R.S. Thorne, Phys. Lett. **B636** 259 (2006).

[7] V.G. Kartvelishvili, A.K. Likhoded and V.A. Petrov, Phys. Lett. **B78** 615 (1978).

[8] F. D. Aaron *et al.* [H1 Collaboration], Eur. Phys. J. **C59** 589 (2009).

[9] H. Jung, Comput. Phys. Commun. **86** 147 (1995); RAPGAP 3.2 program manual unpublished, http://www-h1.desy.de/∼jung/RAPGAP.html.

[10] H. Jung, Proc. 7th DIS Workshop, Nucl. Phys. (Proc. Suppl.) **B79** 429 (1999); H. Jung, Proc. Workshop on Monte Carlo Generators for HERA Physics, 1998-1999, DESY-PROC-1999-02, p.75 arXiv:hep-ph/9908497; H. Jung and G. Salam, Euro. Phys. J. **C19** 351 (2001).

[11] W.K. Tung *et al.*, JHEP **0702** 053 (2007).

[12] M. Ciafaloni, Nucl. Phys. **B296** 49 (1988); S. Catani, F. Fiorani and G. Marchesini, Phys. Lett. **B234** 339 (1990); S. Catani, F. Fiorani and G. Marchesini, Nucl. Phys. **B336** 18 (1990); G. Marchesini, Nucl. Phys. **B445** 49 (1995).

[13] H. Jung, *Procs. of the XII International Workshop on Deep Inelastic Scattering (DIS 2004)*, Strbske Pleso, Slovakia, April 14-18, 2004, Eds. D. Bruncko, J. Ferencei and P. Strizenec, IEP SAS, Kosice, Vol. I, p.299 arXiv:hep-ph/0411287.

[14] GEANT 3, R. Brun *et al.*, CERN-DD/EE/84-1.

[15] B. Andrieu *et al.* [H1 Calorimeter Group], Nucl. Instrum. Meth. **A336** 460 (1993).

[16] W. M. Yao *et al.* [Particle Data Group], J. Phys. **G33** 1 (2006).

[17] J. Burger *et al.*, Nucl. Instrum. Meth. **A279** 217 (1989).

[18] P. Granet it et al. [French-Soviet-collaboration], Nucl. Phys. **B140** 389 (1978).

[19] H1Collaboration, H1prelim-08-072, https://www-h1.desy.de/publications/

[20] J. Pumplin *et al.*, JHEP **07** 012 (2002).

[21] H1Collaboration, H1prelim-08-172, https://www-h1.desy.de/publications/